

---

Faculty of Science

Faculty Publications

---

This is a post-review version of the following article:

Oxygen and iodine adsorption on cesium-precovered Pt(111)

Jakub Drnec, David A. Harrington

December 2014

The final published version of this article can be found at:

<https://doi.org/10.1016/j.susc.2014.06.021>

---

Citation for this paper:

Drnec, J. & Harrington, D.A. (2014). Oxygen and iodine adsorption on cesium-precovered Pt(111). *Surface Science*, 630, 9-15.

<https://doi.org/10.1016/j.susc.2014.06.021>

# Oxygen and iodine adsorption on cesium-precovered Pt(111)

Jakub Drnec, David A. Harrington\*

*Department of Chemistry, University of Victoria, Victoria, British Columbia, V8W 3V6, Canada.*

---

## Abstract

The adsorption behavior of oxygen and iodine on a Cs-precovered Pt(111) surface is studied with Low Energy Electron Diffraction (LEED), thermal desorption spectroscopy (TDS) and work function measurements. TDS shows multiple oxygen desorption states that depend on Cs coverage, with both atomic and molecular oxygen desorbing from the surface. Cs is stabilized by oxygen relative to Cs on Pt(111), and most is retained on the surface until the last oxygen desorbs. Atomic arrangements are proposed for two  $(4 \times 4)$ -Cs,O structures observed by LEED, and these are similar to Cs,I structures with ionic character. At the highest oxygen and Cs coverages, there is evidence for a molecular oxygen state above room temperature. Dosing iodine on Pt(111)-Cs,O results in substitution of O by I in Cs,O islands. Oxygen adsorption on a Cs-saturated Cs monolayer at 295 K causes an initial work function decrease consistent with underlayer adsorption, i.e., with O adsorption below the plane of the Cs atoms. This feature is absent for adsorption on the lower-coverage Pt(111)( $2 \times 2$ )-Cs surface.

*Key words:* Cesium, Iodine, Oxygen, Platinum, Ionic adsorption, Alkali metals, Single crystal surfaces, Pt(111), UHV

---

## 1. Introduction

Coadsorption of alkali metals and small molecules on single-crystal transition-metal surfaces are important model systems to understand the nature of adsorption and interactions between adsorbates, and they have been well studied [1–3]. As electropositive adsorbates, electron transfer to the surface is significant, or there can be electron transfer to electronegative adsorbates, which leads to the interesting possibility of ionic layers. Our work on Cs-modified Pt(111) identified a strongly-bound low-coverage state of  $\text{Cs}^+$  that directly desorbs as the ion [4], and the interaction of this and higher coverage Cs with iodine showed

---

\*Corresponding author. Tel.: +1-250-7217166; Fax: +1-250-7217147

Email addresses: [drnec@esrf.fr](mailto:drnec@esrf.fr) (Jakub Drnec), [dharr@uvic.ca](mailto:dharr@uvic.ca) (David A. Harrington)

evidence for ionic layers [5]. According to Wang et al. [6], only a few hexagonal arrangements are favorable for planar ionic layers on (111) surfaces, and our LEED studies of the Cs-I coadsorption system found such structures. Here we study another electropositive-electronegative coadsorption system, Pt(111)-Cs,O using the Ultra-High Vacuum (UHV) methods of Low Energy Electron Diffraction (LEED), Thermal Desorption Spectroscopy (TDS) and work function (WF) measurements. We compare the Cs-O system with the Cs-I system, and find similar ( $4 \times 4$ ) structures, suggesting that this structure is common for ionic systems. The coadsorption of all three adsorbates is also studied here.

There is other work on Pt(111)-alkali metal coadsorption, with  $O_2$  [7–11], CO [12–14],  $CH_4$  [15] and cyclic hydrocarbons [16]. However, the atomic arrangement and the bonding characteristics of the Cs-O system are not well understood. Multiple oxygen adsorption states are found to exist on the Pt(111)-Cs,O surface, and we discuss how the structures formed are influenced by the ionicity of the bonding. The strong stabilization of Cs on these Cs,O layers relative to Cs on clean Pt, and the possible presence of adsorbed molecular oxygen above room temperature may be significant in Cs-promoted catalysis.

## 2. Experimental

Experiments were performed in a stainless steel UHV chamber equipped with LEED optics (used also for Auger Electron Spectroscopy (AES)) and a Kelvin probe for work function measurements. A quadrupole mass spectrometer with a custom lock-in detection scheme [17] was used for TDS. The detailed experimental setup description can be found in [4].

Crystals of 1 cm dia. from Metal Oxides and Crystals Ltd were polished with diamond paste (Buehler Ltd.) and then oriented by back-Laue diffraction to a (111) plane within  $0.5^\circ$ . Aluminium oxide slurry ( $0.05 \mu\text{m}$ ) was used as a final polishing step.

Before each set of experiments, the crystal was cleaned by  $Ar^+$  bombardment followed by annealing to 1150 K. The reactivity of the crystal surface can be affected by the presence of impurities such as silicon [18]. Therefore, the crystal was periodically annealed for 1 h at 1150 K in a  $5 \times 10^{-7}$  mbar oxygen atmosphere to allow possible contaminants to segregate to the surface and form stable oxides, which were subsequently removed by  $Ar^+$  bombardment [4].

Cs was dosed from a Cs dispenser (SAES Getters, Cs/NF/2.2/12 FT10+10) located 10 cm from the surface. Surfaces were considered insufficiently clean if the work function change to the minimum was less than 4 eV. A custom-built doser, based on a solid-state  $Ag_4RbI_5$  electrochemical cell, was used to dose iodine on the surface [19]. Oxygen was dosed by exposing the crystal to  $1 \times 10^{-7}$  mbar of  $O_2$ . Adsorption temperatures were  $295 \pm 2$  K unless otherwise specified. We observed no temperature-dependent variations in the work function or other data over this range. LEED patterns were taken with 10 nA beam current after cooling from the quoted preparation temperature to 100 K.

Coverages were obtained with AES. Peaks were normalized relative to the Pt peak at 237 eV and then compared to reference structures with known coverages.

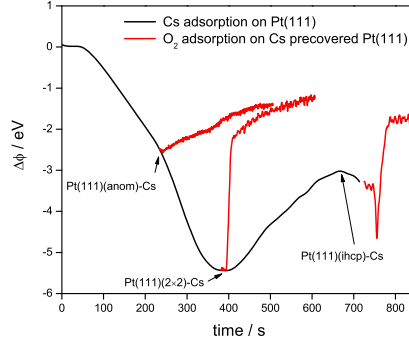


Figure 1: Work function changes for Cs,O coadsorption. The dark (black) curve shows the WF response for Cs. The lighter (red) curves show the WF response to  $O_2$  adsorption on the Cs-precovered surfaces Pt(111)(*anom*)-Cs ( $\theta_{Cs} \approx 0.12 - 0.15$ ), Pt(111)( $2 \times 2$ )-Cs ( $\theta_{Cs} = 0.25$ ) and Pt(111)(*ihcp*)-Cs ( $\theta_{Cs} = 0.41$ ).

For Cs the reference structure was the saturated Cs structure Pt(111)(*ihcp*)-Cs (incommensurate hexagonal close packed,  $\theta_{Cs} = 0.41$  ML); for I the reference structure was the saturated iodine structure Pt(111)( $\sqrt{7} \times \sqrt{7}$ ) $R19.1^\circ$ -I ( $\theta_I = 0.43$  ML) [20–23] and for O, the reference structure was the saturated structure Pt(111)( $2 \times 2$ )-O ( $\theta_O = 0.25$ ) [24, 25].

TD spectra were run at a heating rate of  $5 \text{ K s}^{-1}$ . The lock-in detection scheme is much more sensitive to positive ions leaving the surface than neutrals, which accounts for the enhanced signal for desorption of  $Cs^+$  (anomalous Cs) at  $> 1000 \text{ K}$  in the spectra shown [4].

### 3. Results

#### 3.1. Adsorption of Cs and coadsorption with oxygen or iodine

The work function response for adsorption of Cs on Pt(111) at room temperature is similar to that of other alkali metal/transition metal adsorption systems [26]. The WF initially decreases by about 5 eV (Fig. 1). The break in slope of the WF ("kink") occurring between about  $-1.8$  to  $-3$  eV has been previously assigned to the phase transition from the anomalous ( $Cs^+$ ) to the normal (neutral Cs) adsorption state [4, 27]. After reaching a minimum, corresponding to the Pt(111)( $2 \times 2$ )-Cs structure ( $\theta_{Cs} = 0.25$ ) [4, 5, 14, 28], the WF increases and then levels off as the surface saturates. (After the Cs doser is turned off, the WF slightly decreases, e.g., after 650 s in Fig. 1.) During the WF increase, the surface undergoes several phase transitions [4, 5, 14, 28]. The Pt(111)( $2 \times 2$ )-Cs changes to Pt(111)( $\sqrt{3} \times \sqrt{3}$ )-Cs ( $\theta_{Cs} = 0.33$ ), which further evolves to the saturation incommensurate-hexagonal-close-packed structure, Pt(111)(*ihcp*)-Cs ( $\theta_{Cs} = 0.41$ ).

Starting surface	Dose with	WF change / eV	final $\theta_{\text{Cs}}$	final $\theta_{\text{O}}$ or $\theta_{\text{I}}$
Pt(111)( <i>ihcp</i> )-Cs	O <sub>2</sub>	2.5	$0.32 \pm 0.10$	$1.03 \pm 0.24$
Pt(111)(2 × 2)-Cs	O <sub>2</sub>	3 – 3.5	$0.19 \pm 0.05$	$0.86 \pm 0.24$
Pt(111)( <i>anom</i> )-Cs	O <sub>2</sub>	1	0.15 [4]	0.57 [4]
Pt(111)( <i>ihcp</i> )-Cs	I <sub>2</sub>	2 – 2.5	$0.33 \pm 0.07$ [5]	$0.35 \pm 0.06$ [5]
Pt(111)( <i>anom</i> )-Cs	I <sub>2</sub>	1.5 – 2	$0.10 \pm 0.04$ [4]	$0.37 \pm 0.05$ [4]

Table 1: Summary of final coverages and WF response during O<sub>2</sub> or I<sub>2</sub> dosing on Cs precovered Pt(111) surfaces

At selected Cs coverages, O<sub>2</sub> was dosed and the WF monitored, as shown in Fig. 1, with final coverages given in Table 1. Oxygen adsorption on Pt(111)(*ihcp*)-Cs causes an initial sharp WF decrease followed by an increase of about 2.5 eV to the saturated value. However, this initial decrease disappears if the dosing temperature is decreased from 295 K to 150 K (result not shown), indicating a thermally-activated process. The presence of this decrease was sensitive to surface condition and was more pronounced on better-ordered surfaces, as judged by LEED. At oxygen saturation, the Cs:O coverage ratio determined by AES is 1:3.2 which is close to the 1:3 ratio found by Ayyoob et al. for the saturated Pt(*poly*)-Cs,O surface [10]. When O<sub>2</sub> is dosed on Pt(111)(2 × 2)-Cs or Pt(111)(*anom*)-Cs, the WF shows an increase to saturation. The final WF value after O<sub>2</sub> dosing for all three Cs precovered surfaces is similar: approx. 1.5 – 2 eV lower than the WF of a clean Pt(111) surface.

Table 1 also shows some comparative data for iodine. Independently of the initial Cs coverage, the final value of the work function of the I-saturated Pt(111)-Cs,I surface approaches the work function of the saturated iodine layer (Pt(111)( $\sqrt{7} \times \sqrt{7}$ )R19.1°-I) and the layer has a ( $\sqrt{7} \times \sqrt{7}$ )R19.1° LEED pattern [5, 29, 30]. We will refer to these surfaces as Pt(111)( $\sqrt{7} \times \sqrt{7}$ )R19.1°-Cs,I. In general the shapes of the WF curves for iodine and oxygen were similar, except that the initial decrease in WF for iodine on Pt(111)(*ihcp*)-Cs was less pronounced, about 0.3 eV.

### 3.2. Desorption from Pt(111)-Cs,O

The desorption behavior is complex, with multiple oxygen desorption peaks that depend on the coverages of both oxygen and cesium. To simplify, the thermal desorption spectra are discussed for surfaces prepared by adding oxygen to only two Cs surfaces, the lower coverage Pt(111)(2 × 2)-Cs surface and then the saturation coverage Pt(111)(*ihcp*)-Cs surface. For comparison purposes, the desorption of oxygen from oxygen-dosed Pt(111) is shown in the inset of Fig. 2.

#### 3.2.1. Pt(111)-Cs,O layers from Pt(111)(2 × 2)-Cs

Increasing doses of oxygen onto Pt(111)(2 × 2)-Cs produce surfaces with increasingly complicated TD spectra (Fig. 2). The sharp increase in Cs desorption above 1000 K is the beginning of the peak for desorption of the last 0.15 ML

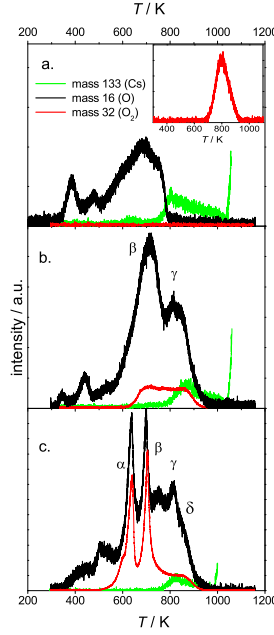


Figure 2: Effect of oxygen coverage on TDS spectra from subsaturated-cesium Pt(111)-Cs,O layers. The layers were prepared by dosing O<sub>2</sub> on Pt(111)(2 × 2)-Cs. O<sub>2</sub> exposures: (a)  $6.7 \times 10^{-5}$  Pa s, (b)  $1.3 \times 10^{-4}$  Pa s, (c) saturated. Inset shows O<sub>2</sub> from fully covered Pt(111)-O, adapted from Ref. [5].

of Cs, the anomalously-adsorbed Cs. The first point to note is that even at the lowest oxygen coverage (Fig. 2a), the Cs is stabilized on the surface, desorbing above 780 K, in contrast to Cs adsorbed on Pt(111) where desorption begins at 600 K (or lower at higher Cs coverages) [4]. Cs desorbs only after the oxygen has been removed from the surface. All the oxygen desorbs as atoms at this coverage, in a series of merged desorption peaks. Assignment of the peaks is difficult, but the highest peak is some combination of the  $\beta$  and  $\gamma$  peaks that are better resolved at higher coverages, e.g., Fig. 2b. Molecular oxygen is now seen desorbing from the surface in the region of both these peaks. For the saturated surface (Fig. 2c), the  $\gamma$  peak has gained a high-temperature shoulder, identified as the  $\delta$  peak. These are more clearly separate at higher Cs coverages (below), but even here the  $\delta$  peak correlates with the final O<sub>2</sub> desorption and there is no corresponding O<sub>2</sub> peak for the  $\gamma$  O desorption peak. The last peak to appear is the  $\alpha$  peak, and both it and the  $\beta$  peak are sharp on the saturated surface, with a similar O:O<sub>2</sub> peak height ratio.

The initial surfaces after O<sub>2</sub> dosing were disordered as judged by LEED, but ordered after heating and partial desorption. Heating to various temperatures between the sharp TDS peaks on the saturated surface, followed by LEED measurements after cooling to 100 K led to the patterns in Fig. 3.

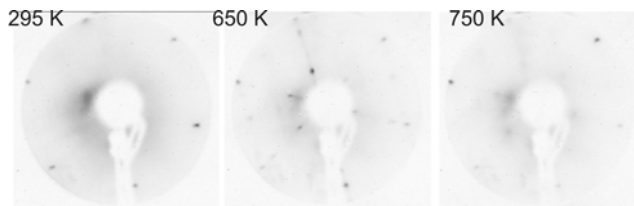


Figure 3: LEED patterns of Pt(111)-Cs,O prepared from Pt(111)( $2 \times 2$ )-Cs by O<sub>2</sub> dosing. Patterns: 295 K (after dosing) diffuse ; 650 K (between the  $\alpha$  and  $\beta$  peaks in Fig. 2c) ( $6 \times 6$ ); 750 K (between the  $\beta$  and  $\gamma$  peaks) weak ( $2 \times 2$ ) with a diffuse background.

### 3.2.2. Pt(111)-Cs,O layers from Pt(111)(*ihcp*)-Cs

TD spectra after dosing oxygen onto the saturated-Cs Pt(111)(*ihcp*)-Cs (Fig. 4) show sharper and higher-intensity Cs and O peaks than from the ( $2 \times 2$ )-dosed surface. The much higher O signals are consistent with the higher coverages measured by AES (sec. 3.1). The O desorption peaks have shifted to higher temperatures, and the  $\gamma$  O peak is much higher relative to the  $\beta$  peak than previously. The  $\gamma$  peak predominates at the lowest oxygen exposure, and it now has a sharp, nearly vertical drop of the type often seen in zero-order desorption peaks. (Instrument sensitivity was reduced for mass 16 in Fig. 4a to avoid overload, so the small mass 16 signal expected to accompany the mass 32 peak at 870 K is lost in the noise.) The  $\gamma$  peak is now clearly separated from the  $\delta$  peak, and only the  $\delta$  peak has an accompanying O<sub>2</sub> desorption peak. It is evident in the sequence that the  $\gamma$  desorption is of atomic oxygen.

At saturation (Fig. 4c), the  $\alpha$  and  $\beta$  peaks have sharpened and a new low-temperature peak has appeared at ca. 350 K. The latter peak has been previously identified as a molecular oxygen state on K-covered surfaces [8] and will not be discussed further. Its O:O<sub>2</sub> peak height ratio is similar to that of the  $\alpha$  and  $\beta$  peaks, and the oxygen in the  $\alpha$  and  $\beta$  states is evidently desorbing as molecular oxygen. The apparently larger ratio for the  $\beta$  peak in 4b can be explained if the  $\beta$  peak is only a small shoulder on the  $\gamma$  peak. In contrast to the surfaces here, there is no molecular O<sub>2</sub> adsorption on clean Pt(111) surface above 150 K [31–34].

A fine structure (673 K) on the trailing edge of the  $\beta$  peak was seen consistently at saturation, but is too small to reliably characterize. The  $\delta$  O<sub>2</sub> peak at 820 K overlaps with the Cs desorption peak, and Cs and O<sub>2</sub> simultaneously desorb at this temperature with an apparent desorption energy of 215 kJ mol<sup>-1</sup> (Redhead analysis,  $k_0 = 10^{13}$  s<sup>-1</sup>). However, there is no evidence for Cs<sub>*x*</sub>O<sub>*y*</sub> cluster desorption in this region: no desorption of CsO (mass 149), CsO<sub>2</sub> (mass 165) or Cs<sub>2</sub>O (mass 282) was measured.

The LEED diffraction patterns observed during desorption from these Pt(111)-Cs,O surfaces are shown in Fig. 5. The ( $4 \times 4$ ) LEED pattern that forms after heating the O<sub>2</sub>-dosed Pt(111)(*ihcp*)-Cs surface to 750 K resembles the LEED from a Pt(111)( $4 \times 4$ )-Cs<sub>2</sub>I layer [5].

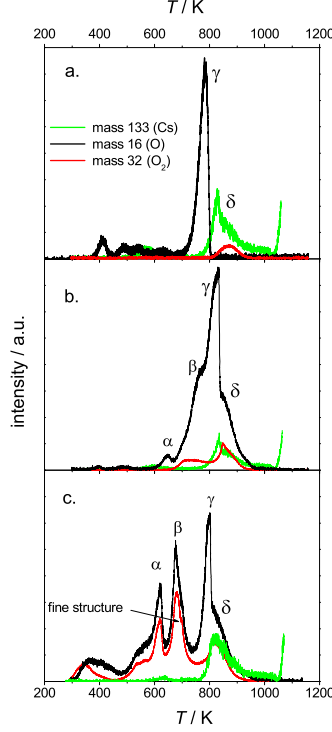


Figure 4: Effect of oxygen coverage on TDS spectra from cesium-saturated Pt(111)-Cs,O layers. The layers were prepared by dosing O<sub>2</sub> on Pt(111)(*ihcp*)-Cs. O<sub>2</sub> exposures: (a)  $1.3 \times 10^{-4}$  Pa s (WF decreased then increased to starting value), (b)  $3.3 \times 10^{-4}$  Pa s (WF above starting value by 0.5 – 1 eV), (c) saturated.

### 3.3. Iodine adsorption on Pt(111)-Cs,O

Iodine exposure to saturation on a Pt(111)-Cs,O layer prepared by exposing the Pt(111)(*ihcp*)-Cs surface to O<sub>2</sub> (until no further change of the WF was observed, ca  $1.3 \times 10^{-3}$  Pa s), leads to a further increase of the WF by 1.5 eV (Fig. 6). AES showed the presence of O, I and Cs on the surface. The peaks for I and O in the AES spectra partially overlap, which makes coverage determination unreliable. If the I<sub>2</sub> and O<sub>2</sub> dosing order is reversed and O<sub>2</sub> is adsorbed on a Pt(111)( $\sqrt{7} \times \sqrt{7}$ )R19.1°-Cs,I layer, no WF change is observed, i.e., the Pt(111)( $\sqrt{7} \times \sqrt{7}$ )R19.1°-Cs,I layer is passivated towards O<sub>2</sub> adsorption. That is, the dosing order during the ternary layer preparation affects the resulting surface structure.

The TDS spectra from a Pt(111)-Cs,O,I layer are shown in Fig. 7. Note that in general I shows little tendency for recombination; for example less than 3% of iodine desorbs from Pt(111)( $\sqrt{7} \times \sqrt{7}$ )R19.1°-I as I<sub>2</sub> (mass 254) [30]. The I and Cs spectra resemble those from Pt(111)-Cs,I layers [5]. A sharp desorption peak of both Cs and I at 600 K is followed by a smaller broad peak with a maximum



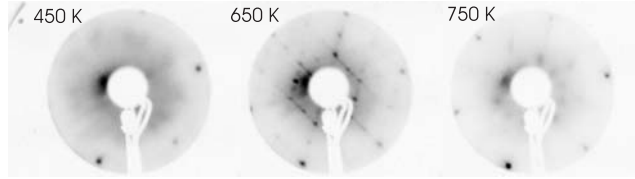


Figure 5: LEED patterns of Pt(111)-Cs,O prepared from Pt(111)(*ihcp*)-Cs by O<sub>2</sub> dosing to saturation. Patterns: 450 K diffuse; 650 K (between the  $\alpha$  and  $\beta$  peaks of the O<sub>2</sub> TD spectrum, Fig. 4c) sharp ( $4 \times 4$ ); 750 K (between the  $\beta$  and  $\gamma$  peaks of the O<sub>2</sub> TD spectrum) ( $4 \times 4$ ) (not very sharp).

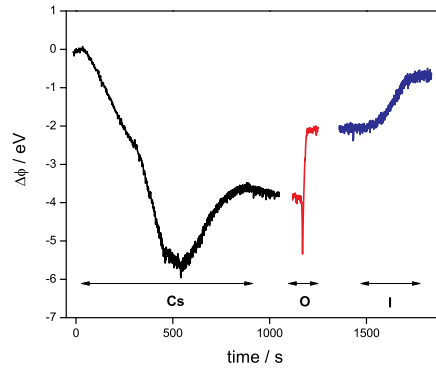


Figure 6: The WF change during the Cs,O,I layer preparation. Left curve (black) shows  $\Delta\phi$  during Cs dosing. Middle (red) curve is the subsequent during oxygen dosing on Pt(111)(*ihcp*)-Cs ( $\theta_{\text{Cs}} = 0.41$ ). Right (blue) curve is the subsequent change during I<sub>2</sub> dosing on the Pt(111)-Cs,O surface.

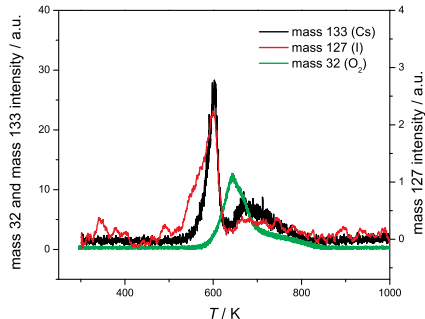


Figure 7: TDS spectra for various masses from Pt(111)-Cs,O,I. The layer was prepared by dosing O<sub>2</sub> on a Pt(111)(*ihcp*)-Cs surface to saturation, followed by I<sub>2</sub> adsorption to saturation. Black curve - mass 133 (Cs), red curve - mass 127 (I) and green curve - mass 32 (O<sub>2</sub>).

around 700 K. These peaks are not related to the I peaks from the Pt(111) surface [35] but indicate concerted removal of Cs and I. The TDS spectra of O<sub>2</sub> (mass 32) dramatically changes compared to the iodine-free Cs,O surface, where multiple peaks are found. Here only one peak with a maximum at 640 K is present, which is not aligned with either the Cs or I desorption peaks.

Exposure of the Pt(111)( $\sqrt{7} \times \sqrt{7}$ )R19.1°-I surface to oxygen showed no WF change and no oxygen adsorption; there was no detectable desorption of O<sub>2</sub> or IO.

#### 4. Discussion

Oxygen coadsorption with alkali metals on transition metal surfaces is important in catalysis and has been extensively studied. Even though some studies on Pt surfaces have been reported [7–11], the bulk of the literature for group 10 transition metal substrates is for coadsorption on Ni surfaces [36–42]. To better understand the structure and bonding arrangements within a Pt(111)-Cs,O layer, we recapitulate what is already known about the coadsorption of alkali metals and oxygen on transition metal surfaces, focusing on the Pt(111) surface.

Studies of oxygen adsorption on Pt(111)-K at 300 K by Pirug et al. [11] using UPS and XPS found two consecutively filled oxygen adsorption states (A and B). The A state, appearing at lower O<sub>2</sub> doses, was assigned to a tightly bound K-O species. It was suggested that this molecule is likely not K<sub>2</sub>O due to the difference in position of the UPS peak relative to oxidized bulk K samples. The B peak, found at higher O<sub>2</sub> doses, was attributed to adsorption of O atoms on bare Pt between K-O islands. This assignment was based on changes in the Pt UPS peak intensity at 0.25 eV, which is characteristic for a clean surface. The coverage of oxygen on the potassium-free part of Pt(111) was calculated as

$\theta_{\text{O}} = 1.1$  or higher [11]. The existence of K-O species was suggested to promote the adsorption of O on the bare Pt surface.

Cassuto et al. [9] found the same A-state UPS peak in their study of  $\text{O}_2$  adsorption on low-coverage Pt(111)-K. However, they suggested that this peak could be safely assigned to  $\text{K}_2\text{O}$  because shifts around 2 – 3 eV are consistent with the bulk values.  $\text{K}_2\text{O}$  can exist in the gas phase [8], but the nature of the K-O interaction on a Pt surface is still unclear. The  $\text{K}_2\text{O}$  stoichiometry is believed to be one of the few stable arrangements in ionic layers, and is important in understanding the formation of 2D ionic crystals [6].

An XPS study by Ayyoob and Hedge [10] of Cs and K adsorption on a Pt(*poly*)-O surface concluded that oxygen is predominantly dissociatively chemisorbed and not necessarily associated with any particular species such as superoxide ( $\text{KO}_2$ ) or peroxide ( $\text{K}_2\text{O}_2$ ). In contrast, Riwan et al. [7] from an angular resolved UPS study of oxygen adsorption on a partially-covered Pt(111)( $2 \times 2$ )-Cs layer tentatively identified two different oxygen species: a peroxo-like  $\text{O}_2^{t-}$ , with  $t \lesssim 2$  at low  $\text{O}_2$  exposures, and  $\text{CsO}_2$  at  $6.5 \times 10^3$  Pa s (50 L)  $\text{O}_2$  exposures.

Our TDS and LEED results from Pt(111)(*ihcp*)-Cs,O have some commonalities with the data measured by Garfunkel et al. for a Pt(111)-K,O layer [8]: i) the O TDS spectrum has multiple sharp desorption peaks, ii) annealing the sample between TDS peaks results in ordering of the surface, and iii) the presence of oxygen thermally stabilizes the adsorbed alkali metal atoms. Interestingly, the spectra taken for  $\theta_{\text{KO}} = 0.65$  and  $\theta_{\text{KO}} = 0.9$  by Garfunkel et al. are very similar to our  $\text{O}_2$  TDS spectra from Pt(111)( $2 \times 2$ )-Cs,O ( $\theta_{\text{Cs}} = 0.24$ , Fig. 2) and Pt(111)(*ihcp*)-Cs,O ( $\theta_{\text{Cs}} = 0.34$ , Fig. 4). That the characteristic shape of the TDS spectra is independent of the different size of the alkali metal atoms is evidence for the same bonding mechanism in both cases, and we use this as a guide for assigning structures.

#### 4.1. Nature of the Pt(111)-Cs,O layers

##### 4.1.1. Low-coverage oxygen state

In the initial stages of oxygen adsorption on Pt(111)(*ihcp*)-Cs or Pt(111)( $2 \times 2$ )-Cs, the oxygen desorbs as atomic oxygen in the  $\gamma$  TDS peak (and  $\beta$  peak for low-coverage oxygen on Pt(111)( $2 \times 2$ )-Cs). This oxygen is strongly attractively interacting with the Cs, and stabilizes it, delaying its desorption to higher than 780 K. The initial work function decrease at the beginning of adsorption (Fig. 1) suggests that the oxygen in the  $\gamma$  state likely adsorbs below the plane of the Cs atoms, at least at high Cs coverages, but caution is required in interpreting work function changes and we defer a more detailed examination of the work function behavior to Sec. 4.2. We identify the  $\gamma$  state with the oxygen A adsorption state of Pirug et al. [11], or the  $\text{K}_2\text{O}$  species of Cassuto et al and Garfunkel et al. [8, 9]. A detailed model for thermal stabilization between oxygen and alkali metal atoms has been proposed by Albano [43]. The same stabilization effect is also seen for Pt(111)-Cs,I, which is another example of a surface layer with strong electrostatic interactions.

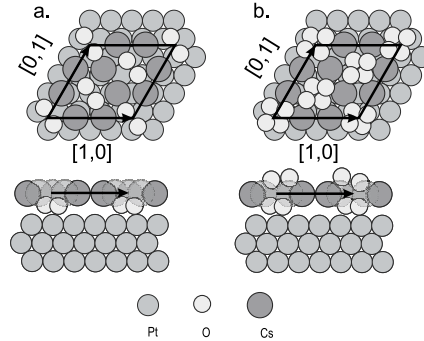


Figure 8: Suggested surface structures for Pt(111)  $(4 \times 4)$ -Cs,O layers after heating to (a) 750 K (CsO); (b) 650 K (CsO<sub>2</sub>). Layer before heating prepared by dosing Pt(111)(*ihcp*)-Cs with oxygen to saturation.

Desorption of oxygen atoms in the  $\gamma$  TDS peak initiates release of the Cs, and the last part of the oxygen and Cs desorb in the  $\delta$  peak (Fig. 4). We propose that the oxygen desorbing in these two peaks originates with the same atomic-oxygen adsorbed state and that the separation into two desorption features occurs dynamically as part of the thermal desorption process. The crowded conditions in the Cs-O layer and the strong Cs-O interaction slow the surface diffusion required for the recombination of oxygen atoms to molecular oxygen, and therefore it desorbs as atomic oxygen in the  $\gamma$  peak. After a critical amount of oxygen is lost, the Cs,O layer reorganizes in a phase transition, as evidenced by zero-order shape of the  $\gamma$  peak with its sharp trailing edge. In the reorganized layer with lower Cs coverage, O can more readily diffuse to recombination sites, likely vacant Pt sites, and desorb as molecular oxygen.

By comparison, low-coverage oxygen ( $< 0.25$  ML) on Pt(111) above 150 K exists as atomic oxygen on the surface [25]. However, it recombines to molecular oxygen on desorption, with second-order desorption kinetics modified by a coverage-dependent activation energy [32].

#### 4.1.2. Pt(111)( $4 \times 4$ )-Cs,O structures

The LEED patterns are sharpest and the coverages most reliably measured for the structures formed by heating the surface prepared by dosing Pt(111)(*ihcp*)-Cs with oxygen to saturation. The low oxygen-coverage  $(4 \times 4)$  structure forms after heating to 750 K, before desorption of the  $\gamma$  oxygen, and the high oxygen-coverage  $(4 \times 4)$  structure forms after heating to 650 K, between the  $\alpha$  and  $\beta$  peaks. Based on the expected ionicity of the Cs-O bond and the same  $(4 \times 4)$  unit cell as found for the ionic Pt(111)( $4 \times 4$ )-Cs<sub>2</sub>I [5] and Pt(111)-K,O [8], we propose that the honeycomb arrangement of Cs atoms within a  $(4 \times 4)$  unit cell is the common structural motif in these systems, and that the coadsorbate oxygen atoms are located in the centers of the hexagons (Fig 8). These ideal structures have Cs coverages of  $6/16 = 0.38$ , close to the experi-

mental coverage of Pt(111)(*ihcp*)-Cs of 0.41. From our oxygen TDS spectra, we estimate that about 1/3 of the O coverage at saturation corresponds to each of  $\alpha$ ,  $\beta$  and  $\gamma$  peaks (Fig. 4). Given that the Cs:O ratio is 1:3.2 at saturation (from AES), ratios of 1:2 at 650 K and 1:1 at 750 K are reasonable. The same Cs:O ratios of 1:2 and 1:1 were also suggested as most probable on Pt(*poly*)-Cs,O surfaces by Ayyoob et al. [10]. Therefore in our proposed arrangements, two (1:1 ratio) or four (1:2 ratio) O atoms, respectively, are located in the center of the hexagons. A unit cell geometry with negative charges located in the center of positively-charged hexagons was identified by Wang et al. [6] as one of the more stable arrangements for 2D ionic layers. If the bonding were more covalent, with more stringent local geometric requirements, the bonding of Cs to I, O and Pt would likely produce very different surface structures for each layer. A high packing density of O is reasonable, because adsorbed O is significantly smaller than adsorbed Cs, and it is well known that high O coverages of up to 2.9 ML can be prepared on Pt surfaces by various techniques [25, 44].

The higher-coverage structure has oxygen in the  $\beta$  adsorption state and is better ordered (Fig. 5). An increase of the Cs-O and Cs-Pt bond polarization with increasing oxygen coverage is expected. Cs atoms will become more positive, which is in accordance with the observations from alkali-metal/oxygen/Ni surfaces [39, 40]. The  $\beta$  state desorbs as molecular oxygen, and the oxygen atoms in the proposed structure may be close enough for some bonding, but it may just be that the proximity of the atoms facilitates recombination.

#### 4.1.3. Other structures

Additional oxygen on the Pt(111)(*ihcp*)-Cs surface populates the  $\alpha$  state. It is tempting to assign oxygen in the  $\alpha$  adsorption state to atomic oxygen bound to the bare Pt surface between Cs,O islands (the high-coverage B state assigned by Pirug et al.), but we have no direct proof of this. This oxygen desorbs molecularly as would be consistent with adsorbed atomic oxygen desorbing from Pt(111), though the local environment is very different.

At the saturation coverage of oxygen, the oxygen desorbs at 350 K (Fig. 4c) and is assigned to molecularly adsorbed oxygen, based on comparison with the analogous K system [8]. On Pt(111) without Cs, molecular oxygen is only found at temperatures below 150 K [25]. This represents a dramatic stabilization of molecular oxygen by Cs.

On the Pt(111)( $2 \times 2$ )-Cs,O surfaces with lower Cs coverage (0.25 ML), there is less stabilization of the Cs as evidenced by the lower desorption temperatures. There is also less strongly-interacting  $\gamma$  oxygen relative to the  $\beta$  oxygen and this may be due to the freedom of oxygen to bond between Cs atoms in other configurations. This is also reflected in the absence of the initial work function decrease on oxygen adsorption, which suggests there is no longer a requirement for adsorption below the Cs atoms.

#### 4.2. Work function changes and oxygen sublayer adsorption

Adsorption of strongly electronegative oxygen typically increases the work function, consistent with the surface dipoles comprising the electrical double

layer having the negative charge on the oxygen atoms and the positive charge on the metal surface atoms. The simplest explanation of the initial WF decrease observed when  $O_2$  is adsorbed on a  $Pt(111)(ihcp)$ -Cs surface is therefore that the oxygen atom absorbs underneath the Cs atoms. However, the O does not need to be directly below the Cs. Similar to the case of the  $Rh(0001)(\sqrt{3} \times \sqrt{3})R30^\circ$ -Cs,O layer [45], it is possible that O may be located in between Cs atoms but directly interacting with the substrate. Because O atoms are significantly smaller than Cs, the negatively charged O atoms can be located closer to the substrate than the positively-charged Cs, which is sufficient for the WF to decrease. We refer to this situation as sublayer adsorption, and the oxygen atom locations in the proposed  $Pt(111)(4 \times 4)$ -Cs,O structures are compatible with it.

An initial WF decrease on oxygen adsorption has been observed for numerous oxygen/alkali metal/transition metal coadsorption systems ([37, 46, 47] and references therein), but the mechanism is not well understood. Two competing adsorption models explaining this feature have been proposed, one by Rhead [46, 48], and the other by Heskett et al. [47].

For the Rhead model, the structure of the alkali metal layer is a key factor. If the local surface coverage of alkali metal is high enough, oxygen can adsorb under the alkali metal. The sublayer adsorption with negative charges on oxygen below positive charges on the alkali metal atoms explains the sharp initial work function decrease. Once all sub-layer adsorption sites have been occupied, oxygen starts to adsorb on other available sites located either in-plane or above the alkali metal, which causes the WF to increase. Two cases are considered. In type I, the high local alkali-metal coverage is achieved by clusters forming (induced or stabilized by oxygen) in an otherwise dispersed low-density phase. This leads to WF decreases upon oxygen adsorption at coverages well before the work function minimum at coverage  $\theta_{\text{min-alkali}}$ . In type II, the high local alkali metal coverage is achieved by dense 2-D islands that nucleate above a critical coverage, which often coincides with  $\theta_{\text{min-alkali}}$ .

Our oxygen adsorption on  $Pt(111)$ -Cs data can be suitably explained by the type II behavior (Fig. 1). We assume that the  $(2 \times 2)$  Cs structure is insufficiently dense for sublayer oxygen, but the higher-coverage  $Pt(111)(\sqrt{3} \times \sqrt{3})R30^\circ$ -Cs and  $Pt(111)(ihcp)$ -Cs phases provide the densely packed Cs islands to accommodate sublayer oxygen that are required by the theory. The underlayer adsorption only begins after LEED shows the  $Pt(111)(\sqrt{3} \times \sqrt{3})R30^\circ$ -Cs phase, which is after the WF minimum.

The difference in work function adsorption behavior between Cs,I and Cs,O can be explained by the different size of adsorbed atoms. The radii of  $O^-$  or  $O^{2-}$  ions are significantly less than for  $I^-$ . Therefore, oxygen can move more easily through a Cs layer and fit better under the Cs than  $I^-$ , which is similar in size to the  $Cs^+$  ions. The iodine cannot easily penetrate below a Cs layer and therefore the initial decrease of the WF is minimal. A more detailed discussion of planar versus bilayer ionic structures can be found in [5].

The competing model by Heskett et al. [47, 49] explains the initial WF behavior in terms of increased polarization of alkali metal-Pt bonds. In the

initial stages of oxygen adsorption, electronegative O polarizes the alkali metal-Pt bond through an induced electrostatic field and the WF decreases. The progression of induced WF change depends on the interplay between the WF increase due to the O-Pt dipole moment (opposite polarity of the alkali metal-Pt dipole) and the WF decrease due to the further polarization of alkali metal-Pt bonds. Sublayer adsorption is not a requirement in the model, which predicts a decrease in the WF for layers where O is in-plane with or above the alkali metal.

In the Heskett model, the re-polarization of Cs-Pt bond should occur independently of the O position in the unit cell (because it is a field effect). Our observation is that the initial WF decrease for oxygen adsorption on Pt(111)(*ihcp*)-Cs is a thermally activated process. This is more likely for a significant structural arrangement such as for sublayer adsorption than for adsorption in a regular adsorption site, which is typically activationless. Accordingly, we favor the Rhead model over the Heskett model.

#### 4.3. Iodine adsorption on Pt(111)-Cs,O

Dosing iodine on a Pt(111)-Cs,O layer causes the WF to increase without any initial decrease (Fig. 6). As discussed in section 4.2, this means that iodine adsorbs on or in the Cs,O layer, but not underneath it. From the WF measurement alone, it cannot be established if oxygen simultaneously desorbs during iodine adsorption. However, O<sub>2</sub> TDS spectra clearly show that a significant amount of oxygen is left on the surface after I<sub>2</sub> dosing (Fig. 7). The LEED pattern from a Pt(111)-Cs,O,I surface is diffuse, showing the lack of long range order.

By comparing I TDS (mass 127) from Pt(111)-Cs,I,O with the I TDS from Pt(111)-Cs,I [5], the bonding properties of iodine in the layer can be examined. The Cs and I signals from the Pt(111)-Cs,O,I layer resemble those from Pt(111)( $\sqrt{7} \times \sqrt{7}$ )R19.1°-Cs,I with a characteristic sharp peak around 500 K. It is therefore concluded that most of the iodine is interacting with Cs in the layer; the oxygen presence does not influence I or Cs desorption, and the oxygen interacts only weakly with both Cs and I.

We suggest that the oxygen in the Pt(111)-Cs,I,O is bonded to the Pt substrate and is located between Cs,I islands. This suggestion is mainly based on the significant similarities between O<sub>2</sub> TDS spectra from Pt(111)-Cs,I,O and from Pt(111)-O at high coverage O ( $\theta_O = 1.26$ ) [25]. The spectrum of Weaver et al. [25] is similar to our measured spectrum, showing that O in the Cs,I,O layer most likely desorbs from dense islands of O which are not interacting with Cs,I. Similar surface structures for K,O and O islands were used to explain UPS experimental results by Pirug et al. [11] (Sec. 4). Adsorption between Cs,I islands was also observed for oxygen adsorption onto a Pt(111)(4×4)-Cs<sub>2</sub>I surface [5].

However, other explanations are possible. Iodine could adsorb on top of the layer, effectively trapping the oxygen underneath. This would also result in a work function increase due to the iodine electronegativity. When the surface is heated, the Cs and I desorption at 500 K would allow oxygen originally trapped

below the layer to leave the surface in the sharp peak resembling the desorption from Pt(111)-O surface. This mechanism could also lead to the TDS spectrum in Fig. 6.

## 5. Conclusions

Coadsorption of oxygen and Cs on Pt(111) results in complex structures, in which oxygen stabilizes Cs on the surface. The initially-adsorbed oxygen at higher Cs coverages is associated with a decrease in work function which is associated with sublayer adsorption. Cs,O structures show a  $(4 \times 4)$  unit cell in common with the Cs,I and K,O coadsorption systems and thermal desorption spectra are similar to those for K,O, which suggests that ionic aspects of these systems determine the structures. A honeycomb arrangement of Cs atoms is proposed, in which the oxygen atoms fill the centres of the hexagons. At the highest Cs and O coverages studied here, molecular oxygen is found on the surface, even above room temperature.

For iodine adsorption on Pt(111)-Cs,O, we suggest that because iodine interacts more strongly with cesium than oxygen, oxygen is replaced by I in the Cs,O layer. The resulting surface consists of Cs,I islands with oxygen adsorbed in between these islands. Oxygen desorption is not affected by the presence of the coadsorbed Cs,I islands.

## 6. Acknowledgements

This work was financially supported by the Natural Sciences and Engineering Research Council (NSERC) of Canada and the University of Victoria.

## References

- [1] H. Bonzel, Surface Science Reports 8 (1988) 43 – 125.
- [2] R. Diehl, R. McGrath, Surf. Sci. Rep. 23 (1996) 43–171.
- [3] A. Politano, G. Chiarello, G. Benedek, E. Chulkov, P. Echenique, Surface Science Reports 68 (2013) 305 – 389.
- [4] J. Drnec, D. A. Harrington, Surf. Sci. 603 (2009) 2005 – 2014.
- [5] J. Drnec, D. A. Harrington, Surf. Sci. 604 (2010) 2106–2115.
- [6] J.X.Wang, I. K. Robinson, J. E. DeVilbiss, R. Adzic, J. Phys. Chem. B 104 (2000) 7951–7959.
- [7] R. Riwan, C. Papageorgopoulos, J. Cousty, Surf. Sci. 251/252 (1991) 1086–1090.
- [8] E. L. Garfunkel, G. A. Somorjai, Surf. Sci. 115 (1982) 441–454.



- [9] A. Cassuto, S. Schmidt, M. Mane, Surf. Sci. 284 (1993) 273–280.
- [10] M. Ayyoob, M. S. Hedge, Surf. Sci. 133 (1983) 516–532.
- [11] G. Pirug, H. P. Bonzel, G. Broden, Surf. Sci. 122 (1982) 1–20.
- [12] J. E. Crowel, E. I. Garfunkel, G. A. Samorjai, Surf. Sci. 121 (1982) 303–320.
- [13] L. Whitman, W. Ho, J. Chem. Phys. 90 (1989) 6018–6025.
- [14] M. Tushaus, P. Gardner, A. M. Bradshaw, Langmuir 9 (1993) 3491–3496.
- [15] T. Kondo, T. Sasaki, S. Yamamoto, J. Chem. Phys. 116 (2002) 7673–7684.
- [16] J. M. Davidsen, F. C. Henn, G. K. Rowe, C. T. Campbell, J. Phys. Chem. 95 (1991) 6632–6642.
- [17] S. A. Furman, M. Labayen, R. G. Dean, D. A. Harrington, J. Vac. Sci. Technol., A 19 (2001) 1032–1033.
- [18] K. Griffiths, D. Bonnett, Surf. Sci. 177 (1986) 169–190.
- [19] S. A. Furman, D. A. Harrington, J. Vac. Sci. Technol., A 14 (1996) 256–257.
- [20] T. E. Felter, A. T. Hubbard, J. Electroanal. Chem. 100 (1979) 473 – 491.
- [21] B. C. Schardt, S.-L. Yau, F. Rinaldi, Science 243 (1989) 1050–1053.
- [22] S. C. Chang, S. L. Yau, B. C. Schardt, M. J. Weaver, J. Phys. Chem. 95 (1991) 4787–4794.
- [23] M. Saidy, K. A. R. Mitchell, S. A. Furman, M. Labayen, D. A. Harrington, Surf. Rev. Lett. 6 (1999) 871–881.
- [24] A. Szabo, M. Kiskinova, J. T. Yates, J. Chem. Phys. 90 (1989) 4604–4612.
- [25] J. F. Weaver, J.-J. Chen, A. L. Gerrard, Surf. Sci. 592 (2005) 83–103.
- [26] M. W. Roberts, C. S. McKee, Chemistry of the Metal-Gas Interface, Oxford University Press, New York, 1978.
- [27] J. Lehmann, P. Roos, E. Bertel, Phys. Rev. B 54 (1996) R2347–R2350.
- [28] J. Cousty, R. Riwan, Surf. Sci. 204(1-2) (1988) 45–56.
- [29] S. K. Jo, J. White, Surf. Sci. 261 (1992) 111 – 117.
- [30] S. A. Furman, Surface Chemistry of Iodine on Platinum(111), Ph.D. thesis, University of Victoria, 1998.
- [31] H. Steininger, S. Lehwald, H. Ibach, Surf. Sci. 123 (1982) 1 – 17.
- [32] C. Campbell, G. Ertl, H. Kuipers, J. Segner, Surf. Sci. 107 (1981) 220 – 236.

- [33] N. R. Avery, Chem. Phys. Lett. 96 (1983) 371 – 373.
- [34] P. D. Nolan, B. R. Lutz, P. L. Tanaka, J. E. Davis, C. B. Mullins, J. Chem. Phys. 111 (1999) 3696–3704.
- [35] M. Labayen, S. A. Furman, D. A. Harrington, Surf. Sci. 525 (2003) 149–158.
- [36] A. Politano, V. Formoso, G. Chiarello, Appl. Surf. Sci. 254 (2008) 6854 – 6859.
- [37] P. Finetti, M. Scantlebury, R. McGrath, F. Borgatti, M. Sambi, L. Zaratini, G. Granozzi, Surf. Sci. 461 (2000) 240–254.
- [38] Q. B. Lu, R. Souda, D. J. O’Connor, B. V. King, Phys. Rev. Lett. 77 (1996) 3236–3239.
- [39] T. Ikari, S. Arikado, K. Kameishi, H. Kawahara, K. Yamada, A. Watanabe, M. Naitoh, S. Nishigaki, Appl. Surf. Sci. 252 (2006) 5424 – 5427.
- [40] D. Pacilè, M. Papagno, G. Chiarello, L. Papagno, E. Colavita, Surf. Sci. 558 (2004) 89 – 98.
- [41] A. Cupolillo, G. Chiarello, S. Scalese, L. S. Caputi, L. Papagno, E. Colavita, Surf. Sci. 415 (1998) 62 – 69.
- [42] S. Murray, D. Brooks, F. Leibsle, R. Diehl, R. McGrath, Surf. Sci. 314 (1994) 307 – 314.
- [43] E. V. Albano, J. Chem. Phys. 85 (1986) 1044–1051.
- [44] D. H. Parker, M. E. Bartram, B. E. Koel, Surf. Sci. 217 (1989) 489–510.
- [45] H. Over, H. Bludau, M. Skottke-Klein, W. Moritz, G. Ertl, Phys. Rev. B 46 (1992) 4360–4363.
- [46] G. E. Rhead, Appl. Surf. Sci. 47 (1991) 35–42.
- [47] X. S. D Heskett, D Tang, K. D. Tsuei, J. Phys.: Condens. Matter 5 (1993) 4601–4610.
- [48] G. E. Rhead, Surf. Sci. 203 (1988) L663–L671.
- [49] D. Heskett, D. Tang, X. Shi, K. D. Tsuei, Chem. Phys. Lett. 199 (1992) 138–143.